Tuning the Thermal Stability of Molecular Precursors for the Nonhydrolytic Synthesis of Magnetic MnFe$_2$O$_4$ Spinel Nanocrystals

Qing Song,[†,‡] Yong Ding,[§] Zhong Lin Wang,[§] and Z. John Zhang*[,†]

School of Chemistry and Biochemistry and School of Materials Science and Engineering,
Georgia Institute of Technology, Atlanta, Georgia 30332

Variations on thermal stabilities were studied when the ligands of coordination compounds of manganese (II) acetylacetonate (Mn(acac)$_2$) and iron (III) acetylacetonate (Fe(acac)$_3$) were substituted with benzoylacetonate (bzac). By replacing the acetylacetonate ligand with the benzoylacetonate ligand, the difference of onset thermal decomposition temperatures can be brought within 15° between Fe(bzac)$_3$ and Mn(bzac)$_2$, which shows the feasibility of tuning thermal stability to produce more suitable molecular precursors for the materials syntheses. The closeness in the decomposition temperatures of these two compounds enables the synthesis of high-quality manganese ferrite, MnFe$_2$O$_4$, nanocrystals with tunable sizes from 3 to 12 nm through a combination of a non-hydrolytic reaction and a seed-mediated growth process. Studies on magnetic properties clearly indicate that superparamagnetic properties such as blocking temperature (T_B) and coercivity (H_C) are strongly dependent on the size of these MnFe$_2$O$_4$ nanocrystals, which is consistent with the Stoner−Wohlfarth single domain theory.

Introduction

Nanoscale magnetic materials have been extensively studied for their novel fundamental properties and for a wide range of technological applications such as magnetic data storage, target drug delivery, ferrofluids, and contrast enhancement in magnetic resonance imaging (MRI).[1−8] Recent advances in the syntheses of colloidal nanocrystals have demonstrated that a nonhydrolytic process in organic solvents at elevated temperatures is an effective approach for the synthesis of high-quality colloidal nanocrystals, which have well-controlled chemical compositions, structures, particle sizes, and size distributions.[9−14] The molecular precursors in such a synthesis process usually are inorganic coordination complexes or organometallic compounds. The chemical design of suitable molecular precursors certainly becomes one of the key factors in the success of nanocrystal synthesis in a variety of thermal decomposition reaction systems. In the case of synthesis of magnetic metal oxide nanocrystals, various molecular precursors have been investigated. For example, several iron-containing molecular precursors including an iron Cupferron complex (FeCup$_3$; Cup = C$_6$H$_5$N(NO)O$^-$, N-nitrosophenylhydroxylamine), iron pentacarbonyl (Fe(CO)$_5$), iron (III) acetylacetonate (Fe-(acac)$_3$), and iron carboxylate complexes have been successfully used to prepare binary iron oxide nanoparticles.[15−19]

In the synthesis of binary metal oxides, the decomposition temperature of a molecular precursor is not critical as long as a suitable organic solvent is available at that temperature. However, to produce ternary metal oxides such as spinel ferrite nanocrystals, MFe$_2$O$_4$ (M = Mn, Co, Ni, Cu, Zn, etc.), usually two types of molecular precursors are required for serving as different metal sources in the synthesis process. Certainly, it is highly desirable that the decomposition temperatures of these two types of molecular precursors are as close as possible to achieve the precise control of chemical composition, particle size, and size distribution of nanocrystals.

We report here how the thermal stability of molecular precursors can be tuned to achieve the nonhydrolytic synthesis of high-quality MnFe$_2$O$_4$ nanocrystals by using Mn

(1) Alivisatos, A. P. *Science* **1996**, *271*, 933.
(2) Leslie-Pelecky, D. L.; Rieke, R. D. *Chem. Mater.* **1996**, *8*, 1770.
(3) Sun, S.; Murray, C. B.; Weller, D.; Folks, L.; Moser, A. *Science* **2000**, *287*, 1989.
(4) Häfeli, U.; Schütt, W.; Teller, J.; Zborowski, M. *Scientific and Clinical Applications of Magnetic Carriers*; Plenum Press: New York, 1997.
(5) Weissleder, R.; Bogdanov, A.; Neuwelt, E. A.; Papisov, M. *Adv. Drug Delivery Rev.* **1995**, *16*, 321.
(6) Weissleder, R. *Nat. Biotechnol.* **2001**, *19*, 316.
(7) Weissleder, R.; Moore, A.; Mahmood, U.; Bhorade, R.; Benveniste, H.; Chiocca, E. A.; Basilion, J. P. *Nat. Med.* **2000**, *6*, 351.
(8) Raj, K.; Moskowitz, B.; Casciari, R. *J. Magn. Magn. Mater.* **1995**, *149*, 174.
(9) Murray, C. B.; Norris, D. J.; Bawendi, M. G. *J. Am. Chem. Soc.* **1993**, *115*, 8706.
(10) Peng, X.; Wickham, J.; Alivisatos, A. P. *J. Am. Chem. Soc.* **1998**, *120*, 5343.
(11) Qu, L.; Peng, Z. A.; Peng, X. *Nano Lett.* **2001**, *1*, 333.
(12) Murray, C. B.; Kagan, C. R.; Bawendi, M. G. *Annu. Rev. Mater. Sci.* **2000**, *30*, 545.
(13) Peng, Z. A.; Peng, X. *J. Am. Chem. Soc.* **2001**, *123*, 1389.
(14) Talapin, D. V.; Rogach, A. L.; Kornowski, A.; Haase, M.; Weller, H. *Nano Lett.* **2001**, *1*, 207.

(15) Rockenberger, J.; Scher, E. C.; Alivisatos, A. P. *J. Am. Chem. Soc.* **1999**, *121*, 11595.
(16) Hyeon, T.; Lee, S. S.; Park, J.; Chung, Y.; Na, H. B. *J. Am. Chem. Soc.* **2001**, *123*, 12798.
(17) Sun, S.; Zeng, H. *J. Am. Chem. Soc.* **2002**, *124*, 8204.
(18) Jana, N. R.; Chen, Y.; Peng, X. *Chem. Mater.* **2004**, *16*, 3931.
(19) Yu, W. W.; Falkner, J. C.; Yavuz, C. T.; Colvin, V. L. *Chem. Commun.* **2004**, 2306.

(II) benzoylacetonate, Mn(bzac)$_2$, and Fe(bzac)$_3$ as precursors. High-quality MnFe$_2$O$_4$ nanocrystals with tunable sizes from about 3 to 12 nm have been synthesized via a combination of nonhydrolytic reaction and seed-mediated growth. The magnetic studies of these MnFe$_2$O$_4$ nanocrystals show typical size-dependent superparamagnetic properties. The blocking temperature and coercivity increase with the increasing size of the MnFe$_2$O$_4$ nanocrystals. As the MnFe$_2$O$_4$ nanocrystal size increases from 4.5 to 12 nm, the blocking temperature rises from 32 to 123 K, and the coercivity at 5 K changes from 171 to 447 Oe, respectively.
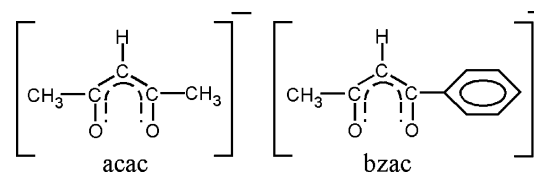
Experimental Procedures

Phenyl ether (99%), oleic acid (90%), oleylamine (>70%), 1,2-hexadecanediol (97%), Fe(acac)$_3$, Mn(acac)$_2$, 1-benzoylacetone (99%), manganese acetate tetrahydrate (99+%), hexane, acetone, and absolute ethanol were purchased from Aldrich Inc. Iron nitrate (98+%) and sodium acetate (99%) were purchased from Fisher Scientific Inc. All chemicals were used as received.

Coordination compounds of Mn(bzac)$_2$ and Fe(bzac)$_3$ were used as precursors in the synthesis of MnFe$_2$O$_4$ nanocrystals. The preparations of these two complexes were adapted from methods in the literature.[20,21] In brief, under N$_2$ gas protection, 5 g of sodium acetate was dissolved in a freshly made 100 mL solution of 0.4 M 1-benzoylacetone in ethanol. Then, the mixture was added dropwise into 100 mL of 0.2 M manganese acetate solution, and a bright yellow precipitate with a little greenish color was gradually formed. After stirring for 8 h, the yellow precipitate was filtrated and washed with ethanol and ether alternatively and dried in a vacuum oven at 40 °C for 8 h. The dry powder of Mn(bzac)$_2$ was stored in a glove box for future use. Fe(bzac)$_3$ was prepared with a similar synthetic procedure while iron acetate was used in place of manganese acetate.

To synthesize MnFe$_2$O$_4$ nanocrystals using Mn(bzac)$_2$ and Fe(bzac)$_3$ as precursors, a mixture of 20 mL of phenyl ether, 1 mmol of Mn(bzac)$_2$, 2 mmol of Fe(bzac)$_3$, 10 mmol of 1,2-hexadecanediol, 3 mL of oleic acid, and 3 mL of oleylamine was heated to 260 °C and kept refluxing at 260 °C for 30 min. After the solution was cooled to room temperature, 20 mL of ethanol was added, and nanocrystals in the form of a black precipitate were collected by either centrifugation or a permanent magnet. These nanocrystals were redispersed in hexane and then reprecipitated by acetone 3 times. The size of the as-synthesized MnFe$_2$O$_4$ nanocrystals was about 3 to 4 nm, which also served as the seeds for further growing the nanocrystals with larger diameters. To prepare larger sized MnFe$_2$O$_4$ nanocrystals, the seed-mediated growth process was employed. By adjusting the ratio of the amount of seed and precursors in solutions, the size of the MnFe$_2$O$_4$ nanocrystals can be tuned up to 12 nm. For example, in the presence of 20 mL of phenyl ether, 1 mmol of Mn(bzac)$_2$, 2 mmol of Fe(bzac)$_3$, 10 mmol of 1-octadecanol, 3 mL of oleic acid, and 3 mL of oleylamine, 8 nm MnFe$_2$O$_4$ nanocrystals were produced by using 60 mg of 4 nm MnFe$_2$O$_4$ nanocrystals as seeds. To further increase the size of the MnFe$_2$O$_4$ nanocrystals, a similar synthetic procedure can be repeatedly used with larger nanocrystals as the seeds. Although larger nanocrystals can also be obtained by increasing the refluxing time in the seed-mediated growth process, the size distribution usually degrades as the refluxing time is extended beyond the common 30 min in our studies.

(20) Berg, E. W.; Truemper, J. T. *J. Phys. Chem.* **1960**, *64*, 487.
(21) Berg, E. W.; Truemper, J. T. *Anal. Chim. Acta* **1965**, *32*, 245.

Scheme 1

acac   bzac

The X-ray diffraction experiments were carried out on a Bruker D8 Advance X-ray diffractometer with Cu Kα radiation. Transmission electron microscopy (TEM) studies were conducted on a JEOL 100C at 100 kV, and high-resolution transmission electron microscopy (HRTEM) was performed on a JEOL 4000 EX at 400 kV. The thermogravimetric analysis (TGA) and differential scanning calorimetry (DSC) measurements were simultaneously measured up to either 400 or 800 °C at a heating rate of 10 °C/min under a dynamic N$_2$ flow using a Netzsch Luxx STA 409 PG. A Superconductor Quantum Interference Devices (SQUID, Quantum Design MPMS--5S) magnetometer was used to conduct magnetic measurements with a magnetic field up to 5 T and a temperature ranging from 5 to 400 K. All samples for magnetic measurements were prepared by dispersing dry MnFe$_2$O$_4$ nanocrystals in eicosane (C$_{20}$H$_{42}$, 99%, Aldrich).

Results and Discussion

Thermal stability studies on coordination compounds have shown interesting and very useful variations when the ligand itself was modified. The variations on the thermal stabilities have been studied when the ligands of coordination compounds of Mn(acac)$_2$ and Fe(acac)$_3$ are substituted with bzac (see Scheme 1). Figure 1 shows the results from the thermal stability studies on Fe(bzac)$_3$ using TGA and DSC recorded simultaneously at a rate of 10 °C/min in a dynamic atmosphere of nitrogen. The thermal decomposition of Fe(bzac)$_3$ occurs at an onset temperature of 221 °C with a continual weight loss up to 55% shown in the TGA curve (Figure 1a). In addition to the exothermic peak at this onset temperature, there is an exothermic peak centered at 228 °C and an endothermic peak at 344 °C displayed in the DSC curve. The results from thermal analysis on Mn(bzac)$_2$ indicate a 5% mass loss from 30 to 120 °C associated with an endothermic event that is characteristic of the loss of absorbed water (Figure 1b). The subsequently small exothermic peak without a mass loss at 142 °C has been attributed to a melting event.[20,22] The main event of up to 50% weight loss begins at 234 °C and is associated with a combination of exothermic and endothermic peaks, which indicates the onset of the thermal decomposition of Mn(bzac)$_2$. These decomposition temperatures are markedly different than the ones for Fe(acac)$_3$ and Mn(acac)$_2$. The thermal decomposition is 186 °C for Fe(acac)$_3$, and Mn(acac)$_2$ decomposes at an onset temperature of 249 °C (see Supporting Information).

Magnetic MnFe$_2$O$_4$ nanocrystals synthesized by using Mn(bzac)$_2$ and Fe(bzac)$_3$ as molecular precursors have a narrow size distribution. Figure 2 displays a monolayer of 12 nm MnFe$_2$O$_4$ nanocrystals with a size distribution of less than 7%. The inset HRTEM clearly shows the atomic lattices, indicating the highly crystalline character of synthesized
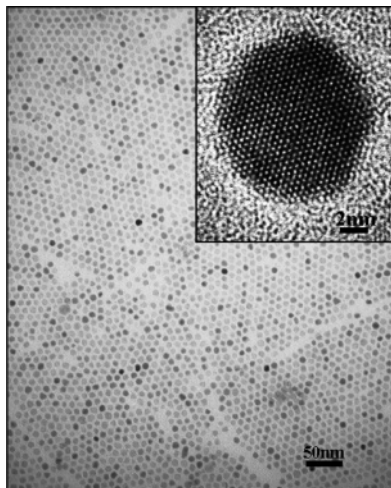
(22) Zhang, Z.; Wong, C. P. *J. Appl. Polym. Sci.* **2002**, *86*, 1572.
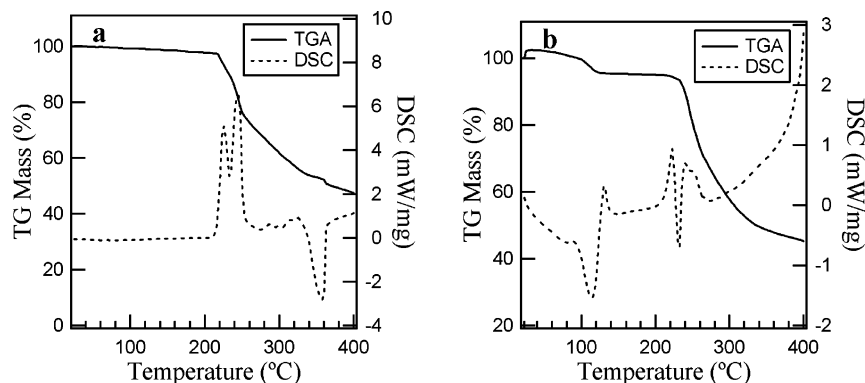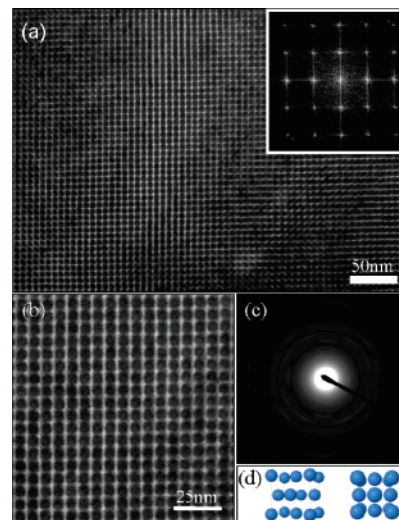
**Figure 1.** TGA and DSC curves for (a) Fe(bzac)$_3$ and (b) Mn(bzac)$_2$.

Figure 2. Typical TEM image of 12 nm MnFe$_2$O$_4$ nanocrystals. Inset is the HRTEM image of a single MnFe$_2$O$_4$ nanocrystal.


Figure 3. (a) fcc superlattice oriented in the [001] direction. Inset is the FFT image with 4-fold symmetry. (b) Partial enlargement of panel a. (c) SAED patterns showing a series of spots instead of ring patterns, indicating the orientation ordering in the superlattice. (d) Model of fcc structure (left) and projection view along the [001] direction (right).
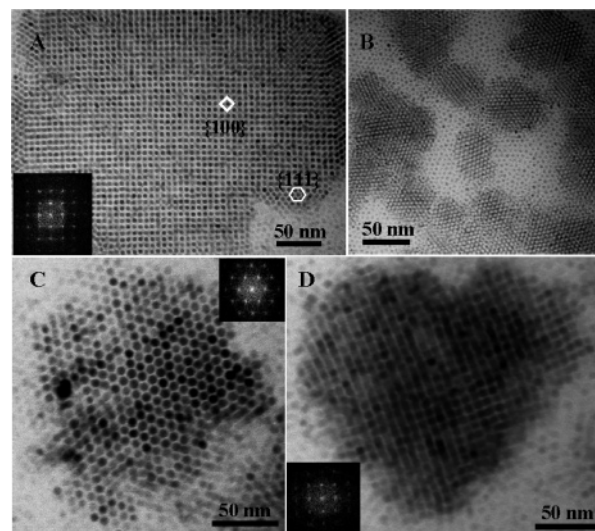

Figure 4. Superlattices formed by (a) 5 nm; inset shows an FFT image with 4-fold symmetry. (b) 3 nm MnFe$_2$O$_4$ nanocrystals. (c) hcp by 8 nm spherical MnFe$_2$O$_4$ nanocrystals; inset shows an FFT image with 6-fold symmetry. (d) Heart-shaped superlattice of 7 nm nanocrystals shows a 4-fold symmetry as indicated by the inset FFT image.

MnFe$_2$O$_4$ nanocrystals. X-ray diffraction studies also confirmed a spinel ferrite structure of as-synthesized MnFe$_2$O$_4$ nanocrystals (see Supporting Information). The chemical composition analysis measured by inductively coupled plasma atomic emission spectroscopy (ICP-AES) has shown a stoichiometry of 1:2 for Mn versus Fe in all synthesized nanocrystals. The MnFe$_2$O$_4$ nanocrystals with smaller sizes have an even narrower size distribution. For example, the size distribution is less than 5% in the MnFe$_2$O$_4$ nanocrystals with a mean size of 4.5 nm. Such a narrow size distribution greatly facilitates the formation of a self-assembled superlattice covering an area of over 1 μm × 1 μm (see Supporting Information). An enlarged part of this superlattice along with the fast Fourier transformation (FFT) image, selected area electron diffraction patterns (SAED), and face-centered cubic (fcc) structure models are displayed in Figure 3a–d, respectively. Differently sized MnFe$_2$O$_4$ nanocrystals have also formed some other interesting superstructures (Figure 4). For example, a heart-shaped superlattice with a 4-fold symmetry is shown in Figure 4d.

The magnetic studies of temperature-dependent magnetization on differently sized MnFe$_2$O$_4$ nanocrystals are shown in Figure 5. The blocking temperatures (T_B) of these various MnFe$_2$O$_4$ nanocrystals increase with the increasing size of the nanocrystals (Figure 5b). As the diameter of the nanocrystals changes from 4.5 to 12 nm, their corresponding blocking temperatures rise from 32 to 123 K. Figure 6 displays the field-dependent magnetization of MnFe$_2$O$_4$

nanocrystals at 5 K. From the inset plot of the hysteresis curves at an expanded scale, it is assured that the MnFe$_2$O$_4$ nanocrystals of all studied sizes show magnetic hysteresis
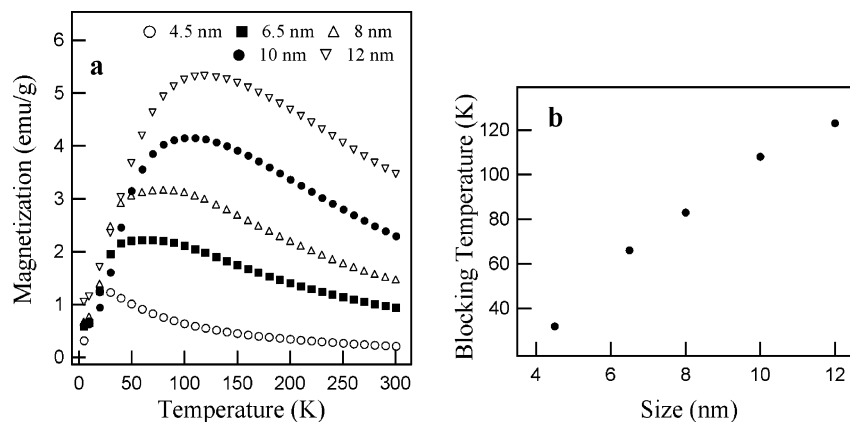
Figure 5. (a) Temperature-dependent magnetization of various sized MnFe$_2$O$_4$ nanocrystals. (b) Blocking temperatures as a function of sizes of MnFe$_2$O$_4$ nanocrystals.
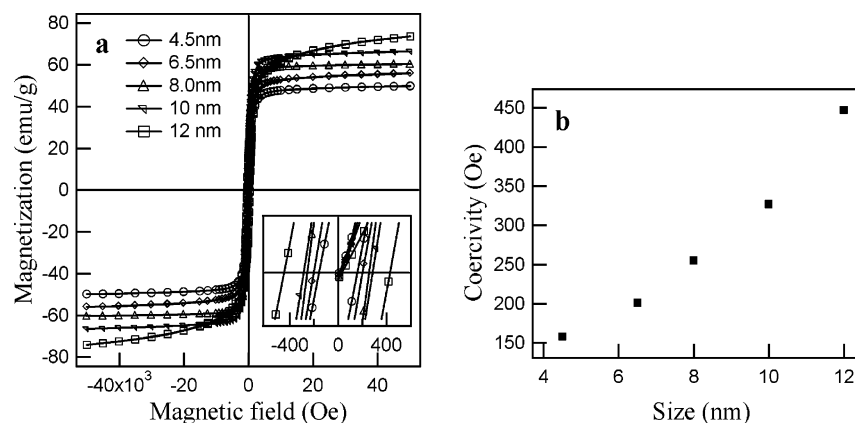
Figure 6. (a) Field-dependent magnetization of various sized MnFe$_2$O$_4$ nanocrystals. (b) Coercivity as a function of sizes of MnFe$_2$O$_4$ nanocrystals.

behavior. The values of coercivity as a function of size are shown in Figure 6b. Clearly, as the size of MnFe$_2$O$_4$ nanocrystals increases, the coercivity of the MnFe$_2$O$_4$ nanocrystals also increases.

Spinel ferrites are complex metal oxides with a flexible chemical composition. The stoichiometry of metal cations can systematically vary as Mn$_{1-x}$Fe$_{2+x}$O$_4$ ($0 < x < 1$) while the spinel crystal structure is still upholding. For the precise control of chemical composition in the synthesis of MnFe$_2$O$_4$ nanocrystals, it is desirable that two types of molecular precursors undergo a simultaneously thermal decomposition at an onset temperature. The closeness of the onset temperatures for the thermal decomposition of Fe(bzac)$_3$ and Mn-(bzac)$_2$ molecular precursors is believed to be critical for the production of controllably sized MnFe$_2$O$_4$ nanocrystals with a precise chemical stoichiometry and narrow size distribution. It certainly enables the control of the concentrations of both metal cation reagents at the nanocrystal nucleation and growth stages. The controllable ratio of reagent concentrations from the almost simultaneous thermal decomposition of multiple molecular precursors should facilitate clean-cut nucleation and growth stages during the nanocrystal formation, which in turn should greatly tighten the size distribution of the nanocrystals. Early studies by LaMer and Dinegar on the formation of monodisperse lyophobic colloids have clearly demonstrated the importance of a distinct nucleation stage and subsequent growth stage upon the particle size distribution.[23]

Such a fine control of the reagent concentrations would be difficult to achieve if using Mn(acac)$_2$ and Fe(acac)$_3$ as molecular precursors. CoFe$_2$O$_4$ nanocrystals in the same spinel ferrite family with MnFe$_2$O$_4$ have been synthesized successfully by the nonhydrolytic reaction using acetylacetonate complexes as precursors, which have decomposition temperatures within 10°.[24] However, the same type of molecular precursors could be problematic for producing MnFe$_2$O$_4$ nanocrystals since the decomposition temperatures for Fe(acac)$_3$ and Mn(acac)$_2$ are more than 60° apart (see Supporting Information). Our repeated efforts in the synthesis of MnFe$_2$O$_4$ nanocrystals using Mn(acac)$_2$ and Fe(acac)$_3$ as molecular precursors have not yielded nanocrystals with satisfactory qualities in terms of controllable chemical composition.

Surely, the thermal properties of coordination complexes are determined by the chemical properties of the central metal and surrounding ligands. The decomposition temperatures of molecular precursors can be raised and lowered by varying the organic ligands in the coordination complexes. The rational substitution of the benzoylacetonate (bzac) ligand for the acetylacetonate (acac) ligand in coordination compounds of Mn(acac)$_2$ and Fe(acac)$_3$ alters their thermal decomposition temperatures in desirable ways. To avoid the difference of more than 60° on the decomposition temperature between Fe(acac)$_3$ and Mn(acac)$_2$, Fe(bzac)$_3$ and Mn-

(23) LaMer, V. K.; Dinegar, R. H. *J. Am. Chem. Soc.* **1950**, *72*, 4847.
(24) Song, Q.; Zhang, Z. J. *J. Am. Chem. Soc.* **2004**, *126*, 6164.

(bzac)$_2$ have been chosen as potentially better molecular precursors for our studies. Purposely substituting the methyl group with a phenyl group in the acac ligand has been designed to reduce the gap in the decomposition temperatures of molecular precursors. Indeed, the new coordination complexes of Fe(bzac)$_3$ and Mn(bzac)$_2$ have thermal decomposition temperatures very close to each other. Clearly, Fe(bzac)$_3$ and Mn(bzac)$_2$ should be the better molecular precursors for the synthesis of MnFe₂O₄ nanocrystals.

The variation in thermal stabilities due to changing the ligands from acac to bzac in the complexes can be attributed to the electronic effect and steric effect of the phenyl group. The phenyl group is a strong π-electron donor, and the electrons are richer around two coordinating oxygen atoms in a bzac ligand as compared to an acac ligand. The metal–ligand bonds that bzac ligands have formed are stronger, and the metal complexes should be more stable because of the increase of the crystal field stabilization energy (CFSE) (Δ) associated with the ligands. Because of such an electronic effect, the decomposition temperatures of Mn(bzac)$_2$ and Fe(bzac)$_3$ should be higher than their counterparts of the acac complexes. Furthermore, the Fe(bzac)$_3$ complex has a common octahedral structure, and Mn(bzac)$_2$ has a tetrahedral structure as its bright yellow color with a little green has indicated.[25] The CFSE is usually much higher in an octahedral complex than a tetrahedral complex for the same central metal and coordinating ligands. Consequently, the electronic effect introduced by the ligand of bzac should be much more profound on increasing the thermal stability from Fe(acac)$_3$ and Fe(bzac)$_3$ than on the Mn(acac)$_2$ and Mn(bzac)$_2$ pair.

On the other hand, steric effects can also affect the thermal stability of the Mn(bzac)$_2$ and Fe(bzac)$_3$ complexes. The phenyl group is a relatively bulky group, and phenyl substitution results in the two oxygen atoms in the bzac ligand being close together as compared to the distance between the two oxygen atoms in the acac ligand.[26−28] For the relatively larger cation Mn^{2+} with a rather crowded tetrahedral structure, the bulkiness of the phenyl group could decrease the thermal stability of Mn(bzac)$_2$, while for the smaller Fe^{3+} with an octahedral coordination, the thermal stability of Fe(bzac)$_3$ could be less susceptible to such a steric effect. On the basis of results from the studies on the thermal stabilities of the Mn(bzac)$_2$ and Fe(bzac)$_3$ complexes, the electronic effect is predominant in the Fe(bzac)$_3$ complex, and the thermal stability of Mn(bzac)$_2$ is mainly controlled by steric effects. Certainly, the decrease in thermal stability of Mn(bzac)$_2$ and an enhancement in the thermal stability of Fe(bzac)$_3$ bring their onset thermal decomposition temperatures very close to make them more or less ideal molecular precursors for the nonhydrolytic synthesis of MnFe₂O₄ nanocrystals. Although the rationale for substituting a methyl group with a phenyl group is speculative, it provides an effective approach for tuning the molecular precursors to satisfy the strict requirements of nonhydrolytic synthesis.

The correlation between the superparamagnetic properties of MnFe₂O₄ nanocrystals and their sizes is consistent with the size dependence of magnetic anisotropy in magnetic nanomaterials according to the Stoner−Wohlfarth theory.[29,30] The magnetic anisotropy is an energy barrier to prevent magnetization varying from one direction to the other. The blocking temperature is the threshold point of thermal activation to overcome such a magnetic anisotropy and to transfer magnetic nanocrystals to the superparamagnetic state. Larger magnetic nanocrystals possess a higher magnetic anisotropy energy, and consequently, a higher thermal energy is required for nanocrystals to become superparamagnetic. Therefore, the blocking temperature increases with the increasing size of the nanocrystals.

The hysteresis in the field-dependent magnetization of the MnFe₂O₄ nanocrystals below the blocking temperature clearly indicates that the magnetic anisotropy serves as an energy barrier to prevent the magnetization orientation of nanocrystals from closely following the switch of the magnetic field direction. The coercivity (H_C) represents the required strength of the magnetic field to overcome the magnetic anisotropy barrier and to allow the magnetization of nanocrystals aligning along the field direction. The coercivity of the magnetic nanocrystal from the Stoner−Wohlfarth theory can be expressed as

$$H_C = 2K/\mu_0 M_S \tag{1}$$

where μ_0 is a universal constant of permeability in free space and M_S is the saturation magnetization of the nanocrystal. As the temperature is below the blocking temperature for the given nanocrystals, the required coercivity for switching the magnetization direction of the nanocrystals certainly increases as the magnetic anisotropy increases. Therefore, the coercivity of the MnFe₂O₄ nanocrystals increases with increasing the nanocrystal size.

Conclusion

We have demonstrated that the thermal stability of molecular precursors is a critical reaction parameter for the size-controlled synthesis of complex multiple-metal oxide nanocrystals. By rational selection of ligands in a molecular precursor through varying the electronic and steric effects, the thermal properties of molecular precursors can be tailored to satisfy the synthetic requirements. Such molecular design approaches for the precursors in general should be useful for the synthesis of more complex metal oxide nanomaterials. The production of high-quality MnFe₂O₄ nanocrystals provides more kinds of magnetic nanocrystals as promising candidates for various practical applications such as MRI

(25) Cotton, F. A.; Wilkinson, G. *Advanced Inorganic Chemistry*, 4th ed.; John Wiley and Sons: New York, 1980; p 665.
(26) Camerman, A.; Mastropaolo, D.; Camerman, N. *J. Am. Chem. Soc.* **1983**, *105*, 1584.
(27) Madsen, G. K. H.; Iversen, B. B.; Larsen, F. K.; Kapon, M.; Reisner, G. M.; Herbstein, F. H. *J. Am. Chem. Soc.* **1998**, *120*, 10040.
(28) Boese, R.; Antipin, M. Y.; Blaeser, D.; Lyssenko, K. A. *J. Phys. Chem. B* **1998**, *102*, 8654.

(29) Stoner, E. C.; Wohlfarth, E. P. *Trans. R. Soc. London, Ser. A* **1948**, *240*, 599.
(30) Stoner, E. C.; Wohlfarth, E. P. *IEEE Trans. Magn.* **1991**, *27*, 3475.

contrast enhancement agents, magnetic probes for biomolecules, and magnetically guided drug delivery.

Supporting Information Available: XRD patterns of $MnFe_2O_4$ nanocrystals, TGA and DSC of $Fe(acac)_3$ and $Mn(acac)_2$, and comparison with $Fe(bzac)_3$ and $Mn(bzac)_2$. TEM image of large-scale self-assembled superlattice formed by 4.5 nm $MnFe_2O_4$ nanocrystals. This material is available free of charge via the Internet at http://pubs.acs.org.

CM070990O